Published in final edited form as:
J Proteome Res. 2010 February 5; 9(2): 1129. doi:10.1021/pr9011359.

Quantitative Proteomic Analysis Reveals the Perturbation of Multiple Cellular Pathways in HL-60 Cells Induced by Arsenite Treatment

Lei Xiong and **Yinsheng Wang***
Department of Chemistry, University of California, Riverside, California 92521-0403

Abstract

Arsenic is ubiquitously present in the environment; it is a known human carcinogen and paradoxically it is also a successful drug for the clinical remission of acute promyelocytic leukemia (APL). The cellular responses induced by arsenite treatment have been investigated for years; however, the precise mechanisms underlying its cytotoxicity and therapeutic activity remain unclear. Here we report the use of mass spectrometry together with stable isotope labeling by amino acids in cell culture (SILAC) for the comparative study of protein expression in HL-60 cells that were untreated or treated with a clinically relevant concentration of arsenite. Our results revealed that, among the 1067 proteins quantified in both forward and reverse SILAC measurements, 56 had significantly altered levels of expression induced by arsenite treatment. These included the up-regulation of core histones, neutrophil elastase, α-mannosidase as well as the down-regulation of fatty acid synthase and protein phosphatase 1α. We further demonstrated that the arsenite-induced growth inhibition of HL-60 cells could be rescued by treatment with palmitate, the final product of fatty acid synthase, supporting that arsenite exerts its cytotoxic effect, in part, via suppressing the expression of fatty acid synthase and inhibiting the endogenous production of fatty acid. The results from the present study offered important new knowledge for gaining insights into the molecular mechanisms of action of arsenite.

Introduction

Arsenic is ubiquitously present in the environment from both natural and anthropogenic sources, especially in groundwater [1]. Arsenic contamination in groundwater has become a widespread public health problem in recent years, causing serious arsenic poisoning to a large population. Chronic arsenic exposure has been associated with increased incidence of various human diseases including atherosclerosis, diabetes, and cancers [2–4]. Despite being a human carcinogen, arsenic trioxide (As_2O_3) has also been used successfully for the clinical remission of acute promyelocytic leukemia (APL) patients [5–7], including those who are resistant to all-*trans* retinoic acid [8]; in 2001, FDA approved the use of arsenic trioxide for APL treatment.

The cellular responses toward arsenite treatment have been extensively studied over the years. Arsenite has been reported to induce the formation of micronuclei and sister chromatid exchanges [9, 10]. It can bind to cysteine sulfhydryl groups in proteins [11], stimulate the formation of oxyradicals [12], inhibit DNA repair, and modulate DNA and histone methylation in mammalian cells [13]. In addition, microarray technique revealed that over one hundred genes in human fibroblast cells were induced or repressed by arsenite treatment [14]. However,

*To whom correspondence should be addressed: Phone: (951) 827-2700. Fax: (951) 827-4713. yinsheng.wang@ucr.edu.

Supporting Information Available: Tables for quantification results and Western blot data for histone proteins. This material is available free of charge via the Internet at http://pubs.acs.org.

microarray analysis does not provide information about the translational regulation of gene expression, which often exhibits a poor correlation with transcript levels owing to the different kinetics of protein translation and turnover [15].

Mass spectrometry (MS)-based proteomics allows for the identification and quantification of a large number of proteins in complex samples. Two-dimensional gel electrophoresis (2-DE) is a traditional technique for studying the effects of drug treatments on protein expression. In 2-DE, quantification is achieved by recording differences in the stained spot intensities of proteins derived from two states of cell populations or tissues [16]. A number of proteomic studies underlying the effect of treatments with different anti-cancer drugs, such as cisplatin [17, 18], etoposide [19] and all-*trans* retinoic acid [20], have been performed by using mass spectrometry for protein identification and 2-DE for protein quantification. The combination 2-DE with mass spectrometry has also been used previously for assessing the arsenite- or arsenic trioxide-induced alterations in protein expression in rat lung epithelial cells [21], TK6 human lymphoblastoid cells [22], immortalized human keratinocytes [23], NB4 human promyelocytic leukemia cells [24], and U266 human multiple myeloma cells [25].

Other than 2-DE, several stable isotope labeling strategies, such as isotope-coded affinity tag [26], isobaric tags for relative and absolute quantitation [27] and stable isotope labeling by amino acids in cell culture (SILAC) [28], have been developed for MS-based analysis of differential protein expression. Among these isotope-labeling strategies, SILAC is a metabolic labeling method, which is simple, efficient, and can facilitate almost complete heavy isotope incorporation. SILAC is very suitable for the comparative study of protein expression in cells with and without drug treatments; accurate results could be obtained with minimal bias, allowing for relative quantification of small changes in protein abundance [28]. In this context, Wiseman et al. [29] used SILAC together with LC-MS/MS and examined the arsenite-induced alterations in the subunit composition of the 26S human proteasome in HEK 293T cells; they found that arsenite treatment led to a 50-fold reduction in the proteasome-associated TRP32.

In the present study, we employed LC-MS/MS, together with SILAC, to assess quantitatively the perturbation of protein expression in cultured HL-60 human acute promyelocytic leukemia cells upon arsenite treatment. We were able to quantify a total of 1067 proteins in both forward and reverse SILAC measurements, among which 56 were significantly altered upon arsenite treatment. The MS quantification results for several target proteins were verified by Western blotting analysis. The identification of proteins perturbed by arsenite treatment sets a stage for understanding the biological pathways affected by arsenite treatment.

Materials and Methods

Materials

Heavy lysine and arginine ([$^{13}C_6$,$^{15}N_2$]-L-lysine and [$^{13}C_6$,$^{15}N_4$]-L-arginine) were purchased from Cambridge Isotope Laboratories (Andover, MA). All chemicals unless otherwise noted were from Sigma (St. Louis, MO).

The rabbit anti-histone H2A, H3, actin and mouse anti-histone H4 antibodies were purchased from Abcam (Cambridge, MA). The mouse anti-histone H2B was from MBL International (Woburn, MA). The rabbit anti-fatty acid synthase was from Cell Signaling (Danvers, MA). HRP-conjugated goat anti-rabbit and anti-mouse IgG secondary antibodies were obtained from Abcam and Santa Cruz Biotechnology (Santa Cruz, CA), respectively.

Cell Culture

HL-60 cells, obtained freshly from ATCC (Manassas, VA), were cultured in Iscove's modified minimal essential medium (IMEM) supplemented with 10% fetal bovine serum (FBS,

Invitrogen, Carlsbad, CA) and penicillin (100 IU/mL). Cells were maintained in a humidified atmosphere with 5% CO_2 at 37°C, with medium renewal at every 2 or 3 days depending on cell density. For SILAC experiments, the IMEM medium without L-lysine or L-arginine was custom-prepared according to the ATCC formulation. The complete light and heavy IMEM media were prepared by the addition of light or heavy lysine and arginine, along with dialyzed FBS (Invitrogen), to the above lysine, arginine-depleted medium. The HL-60 cells were cultured in heavy IMEM medium for at least 5 cell doublings to achieve complete isotope incorporation.

Arsenite Treatment and Cell Lysate Preparation

HL-60 cells, at a density of approximately 7.5×10^5 cells/mL, were collected by centrifugation at 300 g and at 4°C for 5 min, washed twice with ice-cold phosphate-buffered saline (PBS) to remove FBS, and resuspended in FBS-free heavy or light media. In forward SILAC experiment, the cells cultured in light medium were treated with 5 μM arsenite (Sigma) for 24 hrs, whereas the cells cultured in heavy medium were untreated. Reverse SILAC experiments were also performed where the cells cultured in the heavy and light medium were treated with arsenite and mock-treated, respectively (Figure 1). After 24 hrs, the light and heavy cells were collected by centrifugation at 300 g, and washed three times with ice-cold PBS.

The cell pellets were resuspended in the CelLytic™ M cell lysis buffer (Sigma) for 30 min with occasional vortexing. Cell lysates were centrifuged at 12,000 g at 4°C for 30 min, and the resulting supernatants were collected. To the supernatant was subsequently added a protease inhibitor cocktail (Sigma), and the protein concentrations of the cell lysates were determined by using Quick Start Bradford Protein Assay kit (Bio-Rad, Hercules, CA).

SDS-PAGE Separation and In-gel Digestion

The light and heavy cell lysates were combined at 1:1 ratio (w/w), denatured by boiling in Laemmli loading buffer for 5 min and separated by a 12% SDS-PAGE with 4% stacking gel. The gel was stained with Coomassie blue; after destaining, the gel was cut into 20 bands, in-gel reduced with dithiothreitol and alkylated with iodoacetamide. The proteins were digested in-gel with trypsin (Promega, Madison, WI) for overnight, after which peptides were extracted from gels with 5% acetic acid in H_2O and in CH_3CN/H_2O (1:1, v/v). The resulting peptide mixtures were dried and stored at −20°C for further analysis.

Western Blotting

For Western blotting analysis, lysates of the control and arsenite-treated HL-60 cells were prepared following the same procedures as described above. After SDS-PAGE separation, proteins were transferred to a nitrocellulose membrane under standard conditions. A basic transfer buffer containing 10 mM $NaHCO_3$ and 3 mM Na_2CO_3 (pH 9.9) was used for immunoblotting histones. After protein transfer, the membranes were blocked with 5% non-fat milk in PBS-T buffer [PBS solution containing 0.1% (v/v) Tween-20, pH 7.5] for 7 hrs and incubated subsequently with primary antibodies for overnight at optimized dilution ratios. The membranes were washed five times (10 min each) with fresh changes of PBS-T at room temperature. After washing, the membranes were incubated with horseradish peroxidase (HRP)-conjugated secondary antibodies at room temperature for 50 min. The membranes were washed thoroughly with PBS-T for five times (10 min each). The secondary antibody was detected by using ECL Advance Western Blotting Detection Kit (GE Healthcare) and visualized with HyBlot CL autoradiography film (Denville Scientific Inc., Metuchen, NJ).

Fatty Acid Synthase Inhibition and Cell Viability Assay

The palmitate-BSA complex was prepared following a previously published method [30]. Bovine serum albumin (BSA, 5 g) was dissolved in 25 mL of 0.9% NaCl solution with pH being adjusted to 7.4 by NaOH at 5°C, while 4.016 mg sodium palmitate (Sigma) was dissolved in 15 mL of the same NaCl solution at 60°C. The BSA solution was then added to the hot palmitate solution, and the resulting BSA-palmitate mixture was stirred extensively and brought to a volume of 40 mL at a palmitate/BSA molar ratio of 1:5.

HL-60 cells were washed twice with ice-cold PBS to remove FBS, resuspended in FBS-free IMEM medium, and seeded in 6-well plates at a density of ~ 3×10^5 cells/mL. To the cultured cells were added cerulenin or arsenite solutions until their concentrations reached 2.5 μg/mL and 5 μM, respectively. The palmitate-BSA complex solution was added subsequently to the wells containing the control, cerulenin-, or arsenite-treated cells until palmitate concentration was 40 or 80 μM. After 24 or 48 hrs of treatment, cells were stained with trypan blue, and counted on a hemocytometer to measure cell viability.

LC-MS/MS for Protein Identification and Quantification

Online LC-MS/MS analysis was performed on an Agilent 6510 Q-TOF system coupled with an Agilent HPLC-Chip Cube MS interface (Agilent Technologies, Santa Clara, CA). The sample injection, enrichment, desalting, and HPLC separation were carried out automatically on the Agilent HPLC Chip with an integrated trapping column (160 nL) and a separation column (Zorbax 300SB-C18, 75 μm×150 mm, 5 μm in particle size). The peptide mixture was first loaded onto the trapping column with a solvent mixture of 0.1% formic acid in CH_3CN/H_2O (2:98, v/v) at a flow rate of 4 μL/min, which was delivered by an Agilent 1200 capillary pump. The peptides were then separated with a 90-min linear gradient of 2–60% acetonitrile in 0.1% formic acid and at a flow rate of 300 nL/min, which was delivered by an Agilent 1200 Nano pump.

The Chip spray voltage (VCap) was set as 1950 V and varied depending on chip conditions. The temperature and flow rate of the drying gas were set at 325°C and 4 L/min, respectively. Nitrogen was used as the collision gas, and the collision energy followed an equation with a slope of 3 V/100 Da and an offset of 2.5 V. MS/MS experiments were carried out in the data-dependent scan mode with a maximum of five MS/MS scans following each MS scan. The m/z ranges for MS and MS/MS were 300–2000 and 60–2000, and the acquisition rates were 6 and 3 spectra/s, respectively.

Data Processing

Agilent MassHunter workstation software (Version B.01.03) was used to extract the MS and MS/MS data. The data were converted to m/z Data files with MassHunter Qualitative Analysis. Mascot Server 2.2 (Matrix Science, London, UK) was used for protein identification by searching the m/z Data files against the weekly-updated NCBI database. The maximum number of miss-cleavage for trypsin was set as one per peptide. Cysteine carbamidomethylation was set as a fixed modification. Methionine oxidation as well as lysine (+8 Da) and arginine (+10 Da) mass shifts introduced by heavy isotope labeling were considered as variable modifications. The mass tolerances for MS and MS/MS were 50 ppm and 0.6 Da, respectively. Peptides identified with individual scores at or above the Mascot-assigned homology score ($p < 0.01$ and individual peptide score > 30) were considered as specific peptide sequences. The false discovery rates (FDR) determined by decoy database search were less than 0.95%.

Protein quantification was carried out manually and was based on the average ratios of peptide pairs, which was obtained from the intensities of peaks of precursor ions of light and heavy peptides. For those proteins identified with less than 5 peptides, the abundance ratios for ions

of all peptide pairs were used for the quantification; for those proteins identified with more than 5 peptides, five peptide pairs with the highest scores were chosen to determine the protein ratios. The ratio obtained for each individual protein was then normalized against the average ratio for all quantified proteins. This "multi-point" normalization strategy assumes that the ratios for the majority of proteins are not affected by the treatment, facilitating the use of the average ratio of all quantified proteins for re-scaling the data. This has been widely employed to eliminate the inaccuracy during sample mixing introduced by protein quantification with the Bradford assay [31, 32]. The quantification was based on three independent SILAC and LC-MS/MS experiments, which included two forward and one reverse SILAC labeling, and the proteins reported here could be quantified in both forward and reverse SILAC experiments. Some peptides identified in only 1 or 2 trials of QTOF analysis could be quantified in all three trials, where the accurate mass of peptide ions, retention time, and the numbers of isotope-labeled lysine and/or arginine in the peptide were employed as criteria to locate the light/heavy peptide pairs for the quantification.

Results and Discussion

Arsenite Treatment, Protein Identification and Quantification

To gain insights into the molecular pathways perturbed by arsenite treatment, we employed SILAC combined with LC-MS/MS to assess the arsenite-induced differential expression of the whole proteome of HL-60 cells. In this context, clinical pharmacokinetic analyses indicate that the peak plasma arsenite concentration is in the low [33] to high [8, 34] micromolar range for APL patients treated with arsenite. We observed, based on trypan blue exclusion assay, a less than 5% cell death after a 24-hr treatment with 5 μM arsenite, whereas approximately 20% cells were dead if the cells were treated with 7.5 μM arsenite. Thus, we decided to employ 5 μM arsenite for the subsequent experiments to minimize the apoptosis-induced alteration in protein expression.

To obtain reliable results, we carried out the SILAC experiments in triplicate and both forward and reverse SILAC labeling was performed (Figure 1A, see also Materials and Methods). Figure 2 shows example results for the quantification of the peptide GTPLISPLIK from fatty acid synthase, which reveals clearly the down-regulation of this protein in both forward and reverse SILAC experiments (Figure 2A&B). The peptide sequence was confirmed by MS/MS analysis (Figure 2C&D). In addition, we employed serum-free medium in all SILAC-related cell culture experiments to avoid the interactions between arsenite and proteins in the FBS. After cell lysis, SDS-PAGE fractionation, in-gel digestion, LC-MS/MS analysis and database search, we were able to identify 1401 proteins, among which 1380 could be quantified.

Among the quantified proteins, 953 could be quantified in all three measurements, 182 could be quantified in two measurements, and another 245 could be quantified in only one measurement (Figure 1B). We include here only the quantification results for those proteins that could be quantified in all three experiments or in two experiments which include both the forward and reverse SILAC. Together, this gives quantifiable results for 1067 proteins (Table S1).

The distribution of the changes in protein expression levels induced by arsenite treatment is shown in Figure 1C. Among the quantified proteins, 56 display significant changes upon arsenite treatment (the ratio of treated/untreated was greater than 1.5 or less than 0.67), with 21 and 35 being up- and down-regulated, respectively. The quantification results for the proteins with significant changes are summarized in Table 1, and the detailed information about the quantified peptides and ratios for each measurement are listed in Table S2.

Histone proteins are up-regulated upon arsenite treatment

Among the differentially expressed proteins, all four core histones and linker histone H1 were markedly up-regulated in arsenite-treated HL-60 cells (Table S3). In this respect, histone proteins bear many sites of post-translational modifications (PTMs), particularly on their N-terminal tails [35]. Arsenite treatment may perturb the PTMs of histone proteins, which may give rise to inaccurate quantifications of their expression levels. Indeed the exposure of A549 human lung carcinoma cells to arsenite was found to increase H3K9 dimethylation and H3K4 trimethylation while decreasing H3K27 trimethylation [36]. To avoid the inaccurate quantification of histones introduced by arsenite-induced change in PTMs, we chose to use those peptides that do not contain any known PTMs for the quantification [35]. Consistent with what we found from SILAC and LC-MS/MS analysis, Western blotting results also revealed that all core histones were expressed at higher levels in arsenite-treated than in control HL-60 cells (Figure S1).

Although the mechanisms through which the histone proteins are up-regulated upon arsenite treatment remain unknown, many studies showed that arsenite could induce chromosome damage and modulate DNA methylation in mammalian cells [9, 13]. The substantially increased expression of histones might be reflective of the considerable change in chromatin structure induced by arsenite treatment.

Modest down-regulation of heterogeneous nuclear ribonuclear proteins (hnRNPs) and proteins involved in translation

Aside from the considerable upregulation of histone proteins, arsenite treatment also led to a systematic down-regulation of hnRNPs and several important groups of proteins involved in translation (Table S4). In this context, hnRNPs, ribosomal proteins, translation initiation proteins, and translation elongation proteins were all modestly down-regulated upon arsenite treatment (Table S4); the average ratios (treated/untreated) for these four groups of proteins are 0.85, 0.88, 0.82 and 0.82, respectively. These results are in accordance with the previous findings [24, 37] and with the growth inhibition induced by arsentite treatment (*vide infra*).

Arsenite induced the down-regulation of fatty acid synthase (FAS)

Our LC-MS/MS results showed that FAS was down-regulated by approximately 40% upon arsenite treatment. The LC-MS/MS quantification result was validated by Western blotting analysis, which revealed that arsenite treatment gives rise to the dose-dependant decrease in the expression of FAS (Figure 3A). FAS is the sole protein in the human genome capable of reductive synthesis of long-chain fatty acids from acetyl-coenzyme A (acetyl-CoA), malonyl-CoA and NADPH [38]. It has been reported that FAS is highly expressed in human carcinomas [39]. Inhibitors of FAS are selectively toxic to cell lines derived from human malignancies, supporting that cancer cells rely on endogenous fatty acid synthesis for survival and inhibition of FAS may afford an effective route for cancer treatment and prevention [39].

We reason that the decreased expression of FAS may account partly for the cytotoxic effect of arsenite. If this is the case, the arsenite-induced growth inhibition of HL-60 cells should be rescued by palmitate, the end product of FAS. To test this, we assessed whether the proliferation of HL-60 cells is perturbed by arsenite treatment and how this perturbation is affected by externally added palmitate. It turned out that arsenite treatment inhibits the proliferation of HL-60 cells, and palmitate indeed protects, in a dose-dependent fashion, HL-60 cells from arsenite-induced growth inhibition (Figure 3B&C). It was previously observed that the cytotoxicity of cerulenin, a common FAS inhibitor [40, 41], could be abolished by co-administration with exogenous fatty acid [42]. We also observed that the survival of HL-60 cells is compromised upon incubation with cerulenin, which can again be rescued by palmitate (Figure 3D). This result corroborates with the arsenite-induced down-regulation of FAS and

underscores that arsenite may induce cytotoxic effect by inhibiting endogenous fatty acid synthesis through suppressing FAS expression. FAS expression has been found to be controlled by many pathways including Akt [43], and by tumor suppressors and oncogenes, which encompass p53, p63, p73, and H-ras [44, 45]. Further study is needed to unravel the mechanisms involved in the arsenite-mediated down-regulation of FAS.

Arsenite induced the alteration in expression of other important enzymes

Arsenite treatment also gave rise to considerable changes in the expression levels of some other important enzymes, including neutrophil elastase, cathepsin D, α-enolase, α-mannosidase, etc. (Table 1). These proteins play pivotal roles in different cellular pathways, and we would like to discuss some of them in detail.

Neutrophil elastase (NE) is the key protease involved in the cleavage of PML-RARα fusion protein in mouse and human APL cells [46]. The PML-RARα fusion protein generated by the t (15;17) translocation, which is associated with APL, initiated APL when expressed in the early myeloid compartment [46]. Arsenite was shown to induce the degradation of the PML-RARα fusion protein in NB4-S1 cells, which was attributed to the destabilization of lysosome and the subsequent release of hydrolytic enzyme (i.e., cathepsin L) to the cytosol [47]. We observed that NE was up-regulated by approximately 2 fold upon arsenite treatment. Viewing that neutrophil elastase is the dominant PML-RARα cleaving activity in human APL cells [46], our result suggests that arsenite treatment may result in the degradation of the PML-RARα protein through stimulating the expression of NE.

Cathepsin D (CatD) is a lysosomal aspartic protease found in neutrophils and monocytes [48]. CatD is an important cell death mediator [49], and fibroblasts from CatD-deficient mice display more resistance toward etoposide- and adriamycin-induced apoptosis than fibroblasts from the wild-type littermates [50]. Upon arsenite treatment, CatD was up-regulated by 60% (Table 1). The arsenite-induced up-regulation of CatD may also contribute, in part, to the cytotoxic effect of arsenite.

Aside from the enzymes discussed above, there are many other important proteins that are significantly up- or down-regulated by arsenite in HL-60 cells (Table 1). For instance, we found that prothymosin α was substantially up-regulated upon arsenite treatment. This protein is known to compete with transcription factor Nrf2 for binding to the same domain on Keap1, thereby releasing Nrf2 from the Nrf2-Keap1 inhibitory complex [51]. The liberation of Nrf2 can result in the up-regulation of genes involved in defense against oxidative stress and electrophilic attack by binding to the anti-oxidant response elements in promoters of these genes [51–53]. Consistent with this notion, we indeed observed that arsenite treatment led to substantial up-regulation of heme oxygenase 1 (Table 1), a Nrf2 target gene [53], and arsenite is known to induce the formation of reactive oxygen species [12].

Conclusions

Arsenite is an established human carcinogen [54]; on the other hand, it is also a clinically successful anticancer drug for APL treatment [7]. In this study, we employed SILAC, together with LC-MS/MS, and assessed quantitatively the perturbation of protein expression in HL-60 leukemic cells induced by arsenite treatment. Our results revealed that the treatment led to the up- or down-regulation of many important proteins, including histones, fatty acid synthase, neutrophil elastase, cathepsin D, etc. In addition, most ribosomal proteins, translation initiation factors, translation elongation factors, and hnRNPs were modestly down-regulated upon the treatment.

We also confirmed the up- and down-regulation of several proteins by Western blotting analysis. Among the proteins whose expressions are perturbed by arsenite, the down-regulation of fatty acid synthase is of particular importance. In this context, normal adult cells acquire fatty acids mainly from dietary sources and rarely rely on *de novo* fatty acid synthesis because nutritional fatty acids inhibit strongly the expression of the genes involved in fatty acid synthesis [55]. Cancer cells, however, are no longer sensitive to this nutritional signal and instead depend on endogenous fatty acid synthesis to provide vital structural lipids that are required for survival and proliferation [42]. Therefore, fatty acid synthase is substantially up-regulated in many types of tumors and inhibition of this enzyme has been suggested for cancer treatment [39]. Our cell survival data support that the arsenite-induced growth inhibition of HL-60 cells can be rescued by palmitate, the final product of fatty acid synthase. This finding parallels the growth inhibition induced by cerulenin, which is a specific noncompetitive inhibitor of the β-ketoacyl transferase activity of FAS [40, 41]. Thus, our result underscored that the inhibition of endogenous fatty acid synthase may constitute a novel mechanism for arsenite-induced cytotoxic effect.

Further studies about the implications of arsenite-induced perturbation of other proteins may also lead to the discovery of additional molecular pathways that are altered by arsenite and contribute to the arsenite-induced cytotoxicity. The pharmacoproteomic profiling could constitute a valuable tool for the identification of drug-responsive biomarkers for arsenite treatment and establish a molecular basis for developing novel and more effective therapeutic approaches for the treatment of APL and other human cancers.

Supplementary Material

Refer to Web version on PubMed Central for supplementary material.

Acknowledgments

This work was supported by the National Institutes of Health (R01 CA 116522).

Abbreviations

APL	acute promyelocytic leukemia
SILAC	stable isotope labeling by amino acids in cell culture
MS	Mass spectrometry
2-DE	two-dimensional gel electrophoresis
acetyl-CoA	acetyl-coenzyme A
FAS	fatty acid synthase
CatD	cathepsin D
hnRNPs	heterogeneous nuclear ribonuclear proteins

References

1. National Research Council. Arsenic in Drinking Water. National Academy Press; Washington DC: 1999. 2001 update
2. Abernathy CO, Liu YP, Longfellow D, Aposhian HV, Beck B, Fowler B, Goyer R, Menzer R, Rossman T, Thompson C, Waalkes M. Arsenic. Health effects, mechanisms of actions, and research issues. Environ Health Perspect 1999;107:593–597. [PubMed: 10379007]

3. Morales KH, Ryan L, Kuo TL, Wu MM, Chen CJ. Risk of internal cancers from arsenic in drinking water. Environ Health Perspect 2000;108:655–661. [PubMed: 10903620]
4. Cantor KP, Lubin JH. Arsenic, internal cancers, and issues in inference from studies of low-level exposures in human populations. Toxicol Appl Pharmacol 2007;222:252–7. [PubMed: 17382983]
5. Chen GQ, Shi XG, Tang W, Xiong SM, Zhu J, Cai X, Han ZG, Ni JH, Shi GY, Jia PM, Liu MM, He KL, Niu C, Ma J, Zhang P, Zhang TD, Paul P, Naoe T, Kitamura K, Miller W, Waxman S, Wang ZY, deThe H, Chen SJ, Chen Z. Use of arsenic trioxide (As_2O_3) in the treatment of acute promyelocytic leukemia (APL).1. As_2O_3 exerts dose-dependent dual effects on APL cells. Blood 1997;89:3345–3353. [PubMed: 9129041]
6. Chen GQ, Zhu J, Shi XG, Ni JH, Zhong HJ, Si GY, Jin XL, Tang W, Li XS, Xong SM, Shen ZX, Sun GL, Ma J, Zhang P, Zhang TD, Gazin C, Naoe T, Chen SJ, Wang ZY, Chen Z. In vitro studies on cellular and molecular mechanisms of arsenic trioxide (As_2O_3) in the treatment of acute promyelocytic leukemia: As_2O_3 induces NB4 cell apoptosis with downregulation of bcl-2 expression and modulation of PML-RAR alpha/PML proteins. Blood 1996;88:1052–1061. [PubMed: 8704214]
7. Zhu J, Chen Z, Lallemand-Breitenbach V, de The H. How acute promyelocytic leukaemia revived arsenic. Nat Rev Cancer 2002;2:705–13. [PubMed: 12209159]
8. Shen ZX, Chen GQ, Ni JH, Li XS, Xiong SM, Qiu QY, Zhu J, Tang W, Sun GL, Yang KQ, Chen Y, Zhou L, Fang ZW, Wang YT, Ma J, Zhang P, Zhang TD, Chen SJ, Chen Z, Wang ZY. Use of arsenic trioxide (As_2O_3) in the treatment of acute promyelocytic leukemia (APL): II. Clinical efficacy and pharmacokinetics in relapsed patients. Blood 1997;89:3354–60. [PubMed: 9129042]
9. Lerda D. Sister-chromatid exchange (Sce) among individuals chronically exposed to arsenic in drinking-water. Mutat Res 1994;312:111–120. [PubMed: 7510822]
10. Gonsebatt ME, Vega L, Salazar AM, Montero R, Guzman P, Blas J, DelRazo LM, GarciaVargas G, Albores A, Cebrian ME, Kelsh M, OstroskyWegman P. Cytogenetic effects in human exposure to arsenic. Mutat Res 1997;386:219–228. [PubMed: 9219560]
11. Yan H, Wang N, Weinfeld M, Cullen WR, Le XC. Identification of arsenic-binding proteins in human cells by affinity chromatography and mass spectrometry. Analytical chemistry 2009;81:4144–52. [PubMed: 19371058]
12. Liu SX, Athar M, Lippai I, Waldren C, Hei TK. Induction of oxyradicals by arsenic: implication for mechanism of genotoxicity. Proc Natl Acad Sci USA 2001;98:1643–8. [PubMed: 11172004]
13. Kitchin KT. Recent advances in arsenic carcinogenesis: Modes of action, animal model systems, and methylated arsenic metabolites. Toxicol Appl Pharmacol 2001;172:249–261. [PubMed: 11312654]
14. Yih LH, Peck K, Lee TC. Changes in gene expression profiles of human fibroblasts in response to sodium arsenite treatment. Carcinogenesis 2002;23:867–876. [PubMed: 12016162]
15. Wilkins MR, Sanchez JC, Williams KL, Hochstrasser DF. Current challenges and future applications for protein maps and post-translational vector maps in proteome projects. Electrophoresis 1996;17:830–838. [PubMed: 8783009]
16. Klose J, Kobalz U. 2-Dimensional Electrophoresis of Proteins - an Updated Protocol and Implications for a Functional-Analysis of the Genome. Electrophoresis 1995;16:1034–1059. [PubMed: 7498127]
17. Castagna A, Antonioli P, Astner H, Hamdan M, Righetti SC, Perego P, Zunino F, Righetti PG. A proteomic approach to cisplatin resistance in the cervix squamous cell carcinoma cell line A431. Proteomics 2004;4:3246–3267. [PubMed: 15378690]
18. Sinha P, Poland J, Kohl S, Schnolzer M, Helmbach H, Hutter G, Lage H, Schadendorf D. Study of the development of chemoresistance in melanoma cell lines using proteome analysis. Electrophoresis 2003;24:2386–2404. [PubMed: 12874874]
19. Urbani A, Poland J, Bernardini S, Bellincampi L, Biroccio A, Schnolzer M, Sinha P, Federici G. A proteomic investigation into etoposide chemo-resistance of neuroblastoma cell lines. Proteomics 2005;5:796–804. [PubMed: 15682461]
20. Bertagnolo V, Grassilli S, Bavelloni A, Brugnoli F, Piazzi M, Candiano G, Petretto A, Benedusi M, Capitani S. Vav1 modulates protein expression during ATRA-induced maturation of APL-derived promyelocytes: A proteomic-based analysis. J Proteome Res 2008;7:3729–3736. [PubMed: 18642942]
21. Lau AT, He QY, Chiu JF. A proteome analysis of the arsenite response in cultured lung cells: evidence for in vitro oxidative stress-induced apoptosis. Biochem J 2004;382:641–50. [PubMed: 15175009]

22. Tapio S, Danescu-Mayer J, Asmuss M, Posch A, Gomolka M, Hornhardt S. Combined effects of gamma radiation and arsenite on the proteome of human TK6 lymphoblastoid cells. Mutat Res 2005;581:141–52. [PubMed: 15725613]

23. Berglund SR, Santana AR, Li D, Rice RH, Rocke DM, Goldberg Z. Proteomic analysis of low dose arsenic and ionizing radiation exposure on keratinocytes. Proteomics 2009;9:1925–38. [PubMed: 19294697]

24. Zheng PZ, Wang KK, Zhang QY, Huang QH, Du YZ, Zhang QH, Xiao DK, Shen SH, Imbeaud S, Eveno E, Zhao CJ, Chen YL, Fan HY, Waxman S, Auffray C, Jin G, Chen SJ, Chen Z, Zhang J. Systems analysis of transcriptome and proteome in retinoic acid/arsenic trioxide-induced cell differentiation/apoptosis of promyelocytic leukemia. Proc Natl Acad Sci USA 2005;102:7653–8. [PubMed: 15894607]

25. Ge F, Lu XP, Zeng HL, He QY, Xiong S, Jin L. Proteomic and functional analyses reveal a dual molecular mechanism underlying arsenic-induced apoptosis in human multiple myeloma cells. J Proteome Res 2009;8:3006–19. [PubMed: 19364129]

26. Gygi SP, Rist B, Gerber SA, Turecek F, Gelb MH, Aebersold R. Quantitative analysis of complex protein mixtures using isotope-coded affinity tags. Nat Biotechnol 1999;17:994–999. [PubMed: 10504701]

27. Ross PL, Huang YLN, Marchese JN, Williamson B, Parker K, Hattan S, Khainovski N, Pillai S, Dey S, Daniels S, Purkayastha S, Juhasz P, Martin S, Bartlet-Jones M, He F, Jacobson A, Pappin DJ. Multiplexed protein quantitation in Saccharomyces cerevisiae using amine-reactive isobaric tagging reagents. Mol Cell Proteomics 2004;3:1154–1169. [PubMed: 15385600]

28. Ong SE, Blagoev B, Kratchmarova I, Kristensen DB, Steen H, Pandey A, Mann M. Stable isotope labeling by amino acids in cell culture, SILAC, as a simple and accurate approach to expression proteomics. Mol Cell Proteomics 2002;1:376–386. [PubMed: 12118079]

29. Wiseman RL, Chin KT, Haynes CM, Stanhill A, Xu CF, Roguev A, Krogan NJ, Neubert TA, Ron D. Thioredoxin-related Protein 32 is an arsenite-regulated Thiol Reductase of the proteasome 19 S particle. J Biol Chem 2009;284:15233–45. [PubMed: 19349280]

30. Van Harken DR, Dixon CW, Heimberg M. Hepatic lipid metabolism in experimental diabetes. V. The effect of concentration of oleate on metabolism of triglycerides and on ketogenesis. J Biol Chem 1969;244:2278–85. [PubMed: 5783834]

31. Romijn EP, Christis C, Wieffer M, Gouw JW, Fullaondo A, van der Sluijs P, Braakman I, Heck AJR. Expression clustering reveals detailed coexpression patterns of functionally related proteins during B cell differentiation - A proteomic study using a combination of one-dimensional gel electrophoresis, LC-MS/MS, and stable isotope labeling by amino acids in cell culture (SILAC). Mol Cell Proteomics 2005;4:1297–1310. [PubMed: 15961381]

32. Uitto PM, Lance BK, Wood GR, Sherman J, Baker MS, Molloy MP. Comparing SILAC and two-dimensional gel electrophoresis image analysis for profiling urokinase plasminogen activator signaling in ovarian cancer cells. J Proteome Res 2007;6:2105–2112. [PubMed: 17472359]

33. Zhang TD, Chen GQ, Wang ZG, Wang ZY, Chen SJ, Chen Z. Arsenic trioxide, a therapeutic agent for APL. Oncogene 2001;20:7146–53. [PubMed: 11704843]

34. Douer D, Tallman MS. Arsenic trioxide: new clinical experience with an old medication in hematologic malignancies. J Clin Oncol 2005;23:2396–410. [PubMed: 15800332]

35. Lennartsson A, Ekwall K. Histone modification patterns and epigenetic codes. Biochim Biophys Acta 2009;1790:863–8. [PubMed: 19168116]

36. Zhou X, Sun H, Ellen TP, Chen HB, Costa M. Arsenite alters global histone H3 methylation. Carcinogenesis 2008;29:1831–1836. [PubMed: 18321869]

37. Othumpangat S, Kashon M, Joseph P. Sodium arsenite-induced inhibition of eukaryotic translation initiation factor 4E (eIF4E) results in cytotoxicity and cell death. Mol Cell Biochem 2005;279:123–131. [PubMed: 16283521]

38. Wakil SJ. Fatty-acid synthase, a proficient multifunctional enzyme. Biochemistry 1989;28:4523–4530. [PubMed: 2669958]

39. Kuhajda FP. Fatty acid synthase and cancer: New application of an old pathway. Cancer Res 2006;66:5977–5980. [PubMed: 16778164]

40. Funabashi H, Kawaguchi A, Tomoda H, Omura S, Okuda S, Iwasaki S. Binding site of cerulenin in fatty acid synthetase. J Biochem 1989;105:751–5. [PubMed: 2666407]
41. Omura S. The antibiotic cerulenin, a novel tool for biochemistry as an inhibitor of fatty acid synthesis. Bacteriol Rev 1976;40:681–97. [PubMed: 791237]
42. Pizer ES, Wood FD, Pasternack GR, Kuhajda FP. Fatty acid synthase (FAS): A target for cytotoxic antimetabolites in HL60 promyelocytic leukemia cells. Cancer Research 1996;56:745–751. [PubMed: 8631008]
43. Furuta E, Pai SK, Zhan R, Bandyopadhyay S, Watabe M, Mo YY, Hirota S, Hosobe S, Tsukada T, Miura K, Kamada S, Saito K, Iiizumi M, Liu W, Ericsson J, Watabe K. Fatty acid synthase gene is up-regulated by hypoxia via activation of Akt and sterol regulatory element binding protein-1. Cancer Res 2008;68:1003–11. [PubMed: 18281474]
44. Yang YA, Han WF, Morin PJ, Chrest FJ, Pizer ES. Activation of fatty acid synthesis during neoplastic transformation: role of mitogen-activated protein kinase and phosphatidylinositol 3-kinase. Exp Cell Res 2002;279:80–90. [PubMed: 12213216]
45. D'Erchia AM, Tullo A, Lefkimmiatis K, Saccone C, Sbisa E. The fatty acid synthase gene is a conserved p53 family target from worm to human. Cell Cycle 2006;5:750–8. [PubMed: 16582625]
46. Lane AA, Ley TJ. Neutrophil elastase cleaves PML-RAR alpha and is important for the development of acute promyelocytic leukemia in mice. Cell 2003;115:305–318. [PubMed: 14636558]
47. Kitareewan S, Roebuck BD, Demidenko E, Sloboda RD, Dmitrovsky E. Lysosomes and trivalent arsenic treatment in acute promyelocytic leukemia. J Natl Cancer Instit 2007;99:41–52.
48. Benes P, Vetvicka V, Fusek M. Cathepsin D--many functions of one aspartic protease. Crit Rev Oncol Hematol 2008;68:12–28. [PubMed: 18396408]
49. Jaattela M, Cande C, Kroemer G. Lysosomes and mitochondria in the commitment to apoptosis: a potential role for cathepsin D and AIF. Cell Death Differ 2004;11:135–6. [PubMed: 14647234]
50. Wu GS, Saftig P, Peters C, El-Deiry WS. Potential role for cathepsin D in p53-dependent tumor suppression and chemosensitivity. Oncogene 1998;16:2177–83. [PubMed: 9619826]
51. Karapetian RN, Evstafieva AG, Abaeva IS, Chichkova NV, Filonov GS, Rubtsov YP, Sukhacheva EA, Melnikov SV, Schneider U, Wanker EE, Vartapetian AB. Nuclear oncoprotein prothymosin α is a partner of Keap1: implications for expression of oxidative stress-protecting genes. Mol Cell Biol 2005;25:1089–99. [PubMed: 15657435]
52. Hayes JD, McMahon M. Molecular basis for the contribution of the antioxidant responsive element to cancer chemoprevention. Cancer Lett 2001;174:103–13. [PubMed: 11689285]
53. Ishii T, Itoh K, Takahashi S, Sato H, Yanagawa T, Katoh Y, Bannai S, Yamamoto M. Transcription factor Nrf2 coordinately regulates a group of oxidative stress-inducible genes in macrophages. J Biol Chem 2000;275:16023–9. [PubMed: 10821856]
54. Snow ET, Sykora P, Durham TR, Klein CB. Arsenic, mode of action at biologically plausible low doses: what are the implications for low dose cancer risk? Toxicol Appl Pharmacol 2005;207:557–64. [PubMed: 15996700]
55. Sul HS, Wang D. Nutritional and hormonal regulation of enzymes in fat synthesis: studies of fatty acid synthase and mitochondrial glycerol-3-phosphate acyltransferase gene transcription. Annu Rev Nutr 1998;18:331–51. [PubMed: 9706228]

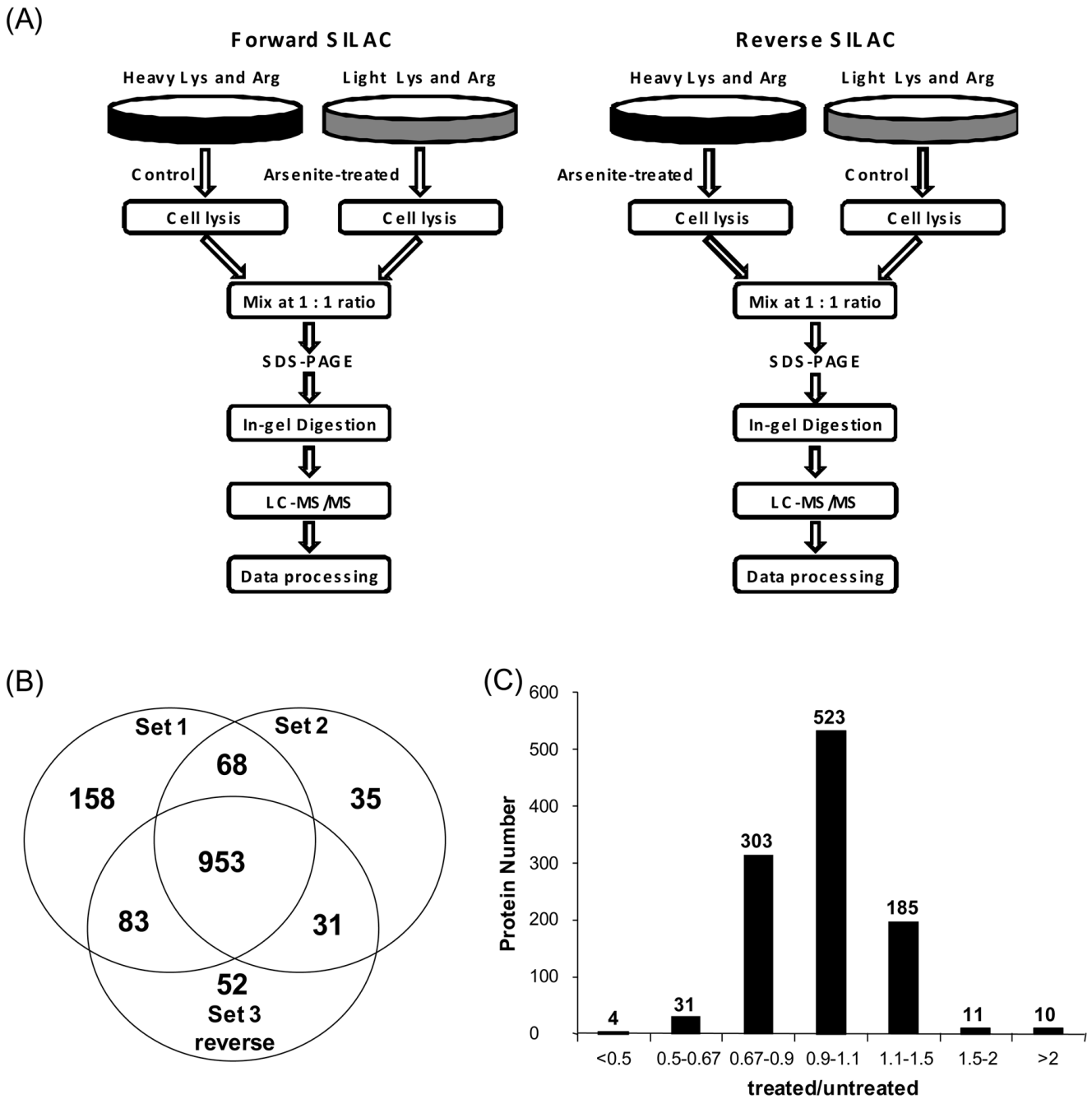

Figure 1.

Forward- and reverse-SILAC combined with LC-MS/MS for the comparative analysis of protein expression in HL-60 cells upon arsenite treatment (A). Shown in (B) and (C) are a summary of the number of proteins quantified from three independent SILAC experiments and the distribution of expression ratios (treated/untreated) for the proteins quantified, respectively. “Set 1” and “Set 2” results were obtained from forward, and “Set 3” results were from reverse SILAC experiments.

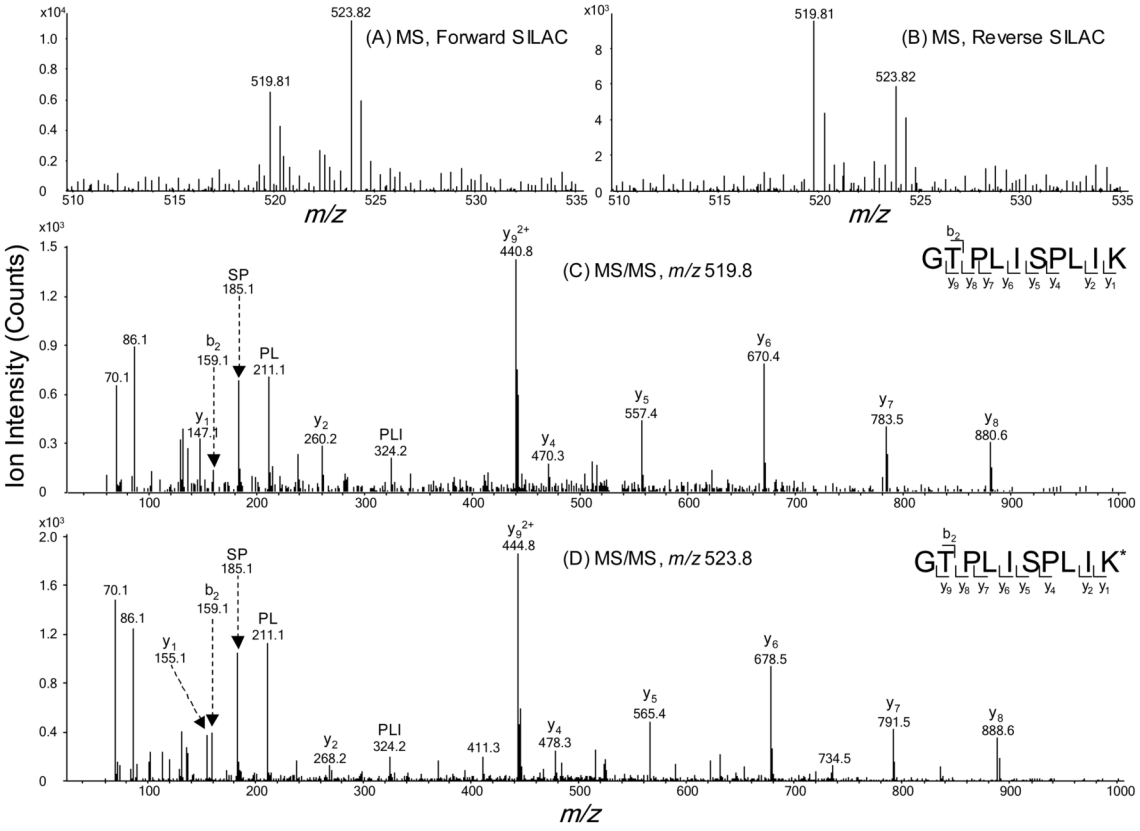

Figure 2.

Example ESI-MS and MS/MS data revealed the arsenite-induced down-regulation of fatty acid synthase. Shown are the MS for the $[M+2H]^{2+}$ ions of FAS peptide GTPLISPLIK and GTPLISPLIK* ('K*' represents the heavy lysine) from the forward (A) and reverse (B) SILAC samples. Depicted in (C) and (D) are the MS/MS for the $[M+2H]^{2+}$ ions of GTPLISPLIK and GTPLISPLIK*, respectively.

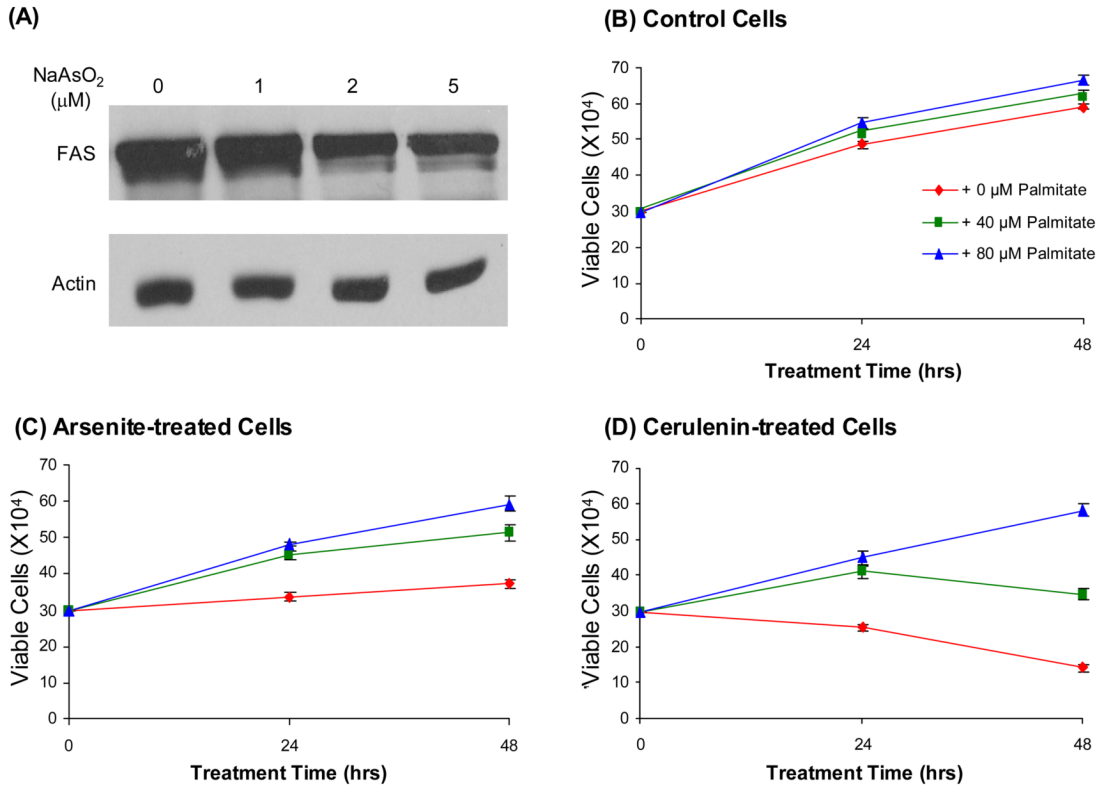

Figure 3.

Western blotting analysis of Fatty acid synthase (FAS) with lysates of untreated HL-60 cells ("control") and HL-60 cells that are treated with 1 μM, 2 μM, or 5 μM of arsenite for 24 hrs (A), and actin was used as the loading control. The viabilities of HL-60 cells after 24 and 48 hrs of treatment with 0, 40, 80 μM palmitate alone (B), or together with 5 μM arsenite (C) or 2.5 μg/mL cerulenin (D).

Table 1

Proteins quantified with more than 1.5 fold changes, with GI numbers, protein names, average ratios and S.D. listed (Peptides used for the quantification of individual proteins are listed in Table S3).

GI Number	Protein Name	Ratio (treated/untreated)
A. Histone and HMG proteins		
11321591	HMG-2	1.65±0.26
968888	HMG-1	1.85±0.07
223582	histone H4	2.41±0.09
386772	histone H3	2.80±0.42
356168	histone H1b	2.76±0.33
1568557	histone H2B	2.98±0.45
510990	histone H2A	4.21±0.54
B. Translation-related proteins		
181969	elongation factor 2	0.54±0.09
38202255	threonyl-tRNA synthetase	0.60±0.12
19353009	Similar to elongation factor 2b	0.62±0.06
4506707	ribosomal protein S25	0.65±0.11
C. hnRNPs		
386547	d(TTAGGG)n-binding protein B39	0.50±0.22
119597533	hnRNP U, isoform CRA_b	0.59±0.01
55958547	hnRNP K	0.66±0.15
D. Enzymes		
531202	spermidine synthase	0.57±0.18
41584442	fatty acid synthase	0.61±0.10
66392203	NME1-NME2 protein	0.64±0.18
1230564	Gu protein	0.64±0.14
2661039	α-enolase	0.65±0.07
190281	protein phosphatase I α subunit	0.66±0.02
4507789	ubiquitin-conjugating enzyme E2L 3 isoform 1	0.67±0.06
5231228	ribonuclease T2 precursor	1.53±0.21
4758504	hydroxysteroid (17-β) dehydrogenase 10 isoform 1	1.56±0.02
4503143	cathepsin D	1.65±0.08
186461558	neutrophil elastase	1.95±0.01
627372	α-mannosidase precursor	2.05±0.24
4504437	heme oxygenase 1	2.32±0.78
12654715	TXNDC5 protein	3.14±0.35
E. Others		
21755073	unnamed protein product	0.42±0.02
119587276	hCG19802, isoform CRA_a	0.47±0.20
35570	unnamed protein product	0.50±0.07
13477237	ZNF607 protein	0.52±0.05
194374111	unnamed protein product	0.57±0.11
35844	unnamed protein product	0.58±0.15

GI Number	Protein Name	Ratio (treated/untreated)
431422	Ran/TC4 binding protein	0.60±0.22
114645930	PREDICTED: nucleosome assembly protein 1-like 1 isoform 9	0.60±0.02
2580550	DEAD box, X isoform	0.61±0.10
122168	HLA class I histocompatibility antigen, B-58 α chain	0.61±0.20
181486	DNA-binding protein B	0.63±0.07
193788267	unnamed protein product	0.63±0.08
801893	leucine-rich PPR-motif containing protein	0.63±0.10
5107666	importin β	0.63±0.20
1235727	unnamed protein product	0.64±0.10
40225729	FUBP1 protein	0.65±0.08
119571409	hCG1643342, isoform CRA_a	0.65±0.03
386777	transplantation antigen	0.66±0.05
1136741	KIAA0002	0.66±0.20
23712	myoblast antigen 24.1D5	0.66±0.08
13569879	acidic (leucine-rich) nuclear phosphoprotein 32 family, member E isoform 1	0.67±0.08
4506773	S100 calcium-binding protein A9	1.53±0.04
9955206	Rho GDP-dissociation factor 2	1.55±0.19
8037945	prothymosin α	1.56±0.02
119239	bone marrow proteoglycan	1.71±0.08
28375485	unnamed protein product	1.81±0.22
4506191	proteasome β10 subunit proprotein	2.21±0.10
32111	unnamed protein product	4.90±0.96